Structure and Dynamic Properties of Nitrile-Butadiene Rubber/Hindered Phenol Composites

Xiu-Ying Zhao,[1] Ya-Jun Cao,[2] Hua Zou,[2] Jing Li,[1] Li-Qun Zhang[1,2]

[1]*Key Laboratory of Preparation and Processing of Novel Polymer Materials, Beijing University of Chemical Technology, Beijing 100029, People's Republic of China*
[2]*Key Laboratory of Ministry of Education on Preparation and Application of Nanomaterials, Beijing University of Chemical Technology, Beijing 100029, People's Republic of China*

Received 21 October 2010; accepted 6 June 2011
DOI 10.1002/app.35043
Published online 22 September 2011 in Wiley Online Library (wileyonlinelibrary.com).

ABSTRACT: Crosslinked nitrile-butadiene rubber (NBR)/hindered phenol composites were successfully prepared by mixing tetrakis [methylene-3-(3-5-ditert-butyl-4-hydroxy phenyl) propionyloxy] methane (AO-60) into NBR with 35% acrylonitrile mass fraction. The structural and mechanical properties of the NBR/AO-60 composites were systematically investigated by using differential scanning calorimeter, XRD, Fourier transform infrared, scanning electronic microscope, dynamic mechanical analyzer, and tensile testing. The results indicated that the AO-60 changed from crystalline form into amorphous form, and most of the AO-60 molecules could be uniformly dispersed in the NBR matrix. The glass transition temperature (T_g) of NBR/AO-60 composites increased gradually with increasing content of AO-60. The increase in T_g could be attributed to the formation of a strong hydrogen bonding network between the AO-60 molecules and the NBR matrix. Unlike the pure NBR, the NBR/AO-60 rubber composites had only one transition with a high loss factor. With increasing content of AO-60, the loss peak shifted to the high temperature region, the loss factor increased from 1.45 to 1.91, and the area under the tan δ versus temperature curve (TA) also showed a significant increase. All these results were ascribed to the good compatibility and strong intermolecular interactions between NBR and AO-60. Furthermore, all NBR/AO-60 composites exhibited higher glass transition temperatures and tensile strength than NBR, and they had other desirable mechanical properties. They have excellent prospects in damping material applications. J Appl Polym Sci 123: 3696–3702, 2012

Key words: hindered phenol; dynamic mechanical properties; hydrogen bonds; damping

INTRODUCTION

Damping materials are also known as vibration attenuation materials. They can convert mechanical vibration energy into thermal energy and eliminate vibration and reduce noise through heat dissipation. Rubber materials are used as damping materials because of their unique viscoelastic properties. The damping mechanism is directly related to the dynamic mechanical relaxation characteristics of the rubber. The damping effect relies on the hysteresis of the rubber. It is because of hysteresis that the cyclic deformation of elongation followed by retraction must overcome the internal friction between the chain segments, leading to energy dissipation.[1] Any external mechanical energy or sound energy will be partly dissipated as heat in this manner. Because rubber has excellent damping properties, rubber-based damping materials are used in a variety of applications including transportation, civil construction, precision instruments, and military equipment.[2,3]

Homopolymers or random copolymers generally have a glass transition region of 20–30°C, therefore the effective damping temperature range for these materials is also 20–30°C.[4] Because rubber generally has a low T_g, and its effective damping temperature range is narrow, pure rubber can satisfy few application requirements without modification. At present, methods like blending, filler reinforcement, and interpenetrating network are used to enhance the rubber damping performance. Although these methods have expanded the effective damping temperature range of the rubber to a certain extent, they actually lead to a significant drop in the damping value.[5–8]

Wu et al.[9,10] proposed a new idea for the design of high-performance damping materials. They added a large amount of small polar organic molecules to chlorinated polyethylene (CPE), which has polar side groups. The strong interaction between CPE and the small molecules results in good damping properties. They studied[11,12] the CPE/AO-80 system

Correspondence to: L.-Q. Zhang (zhanglq@mail.buct.edu.cn).

Contract grant sponsor: National Natural Science Foundation (NSF) of China; contract grant number: 50725310.

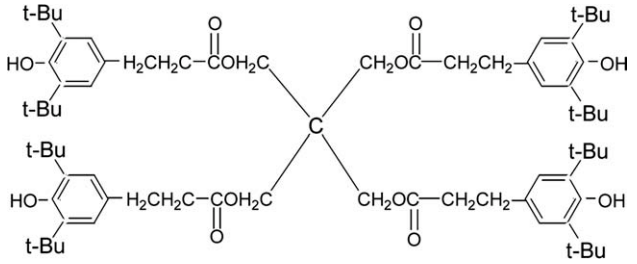

Figure 1 Molecular structure of AO-60.

and found that as a result of the co-existence of the amorphous phase, highly ordered phase, and crystalline phase of AO-80, part of the AO-80 molecules are dispersed in the CPE phase. Most of the AO-80 molecules are enriched because of hydrogen bonding. This structure leads to extremely high damping capacity and good sound absorbance. The resulting composite material is inexpensive and easy to process and has good shape memory, so it has very good prospects in industrial applications.

In an earlier work, we put a hindered phenol of tetrakis [methylene-3-(3-5-ditert-butyl-4-hydroxy phenyl) propionyloxy] methane (AO-60) into nitrile-butadiene rubber (NBR) (with acrylonitrile mass fraction of 41%) for damping modifications.[13–16] We discovered that AO-60 forms an enrichment region in the NBR matrix, and massive hydrogen bonding occurs among the AO-60 molecules as well as between AO-60 and NBR. The hydrogen bonds act as physical crosslinks, and their destruction and formation consume a large amount of energy, resulting in internal energy losses. This composite material presents three relaxation processes, has a large loss peak area, and exhibits high damping performance. An NBR/PVC/hindered phenol composite system with 50 phr of AO-60 displays good comprehensive mechanical properties and twin peaks in the loss factor versus temperature curve.[17,18] However, the compatibility between the small organic molecules and the rubber substrate is poor. In order to improve the compatibility, we experimented with NBR with an acrylonitrile mass fraction of 35% in hope of obtaining composite materials with good compatibility and outstanding damping performance.

EXPERIMENTAL

Materials

NBR (N230s), which has an acrylonitrile percentage of 35 wt % and is used as the matrix in this study, was obtained from Japan Synthetic Rubber Co., Ltd. (Tokyo, Japan). The AO-60 (KY-1010), which is in the form of crystalline powder and used as a functional additive here, was provided by Beijing Additive Research Institute (Beijing, China). The chemical structure and scanning electronic microscope (SEM) image of AO-60 are shown in Figures 1 and 2, respectively. Other chemicals/ingredients were all purchased in China. All materials were used without further purification.

Sample preparation

NBR/AO-60 composites were prepared according to the following procedure: (1) After the as-received NBR was kneaded on a two-roll mill (roll diameter 152.4 mm) at room temperature for 3 min, AO-60 (crystalline power) was added in the NBR/AO-60 ratios of 100/0, 100/20, 100/40, 100/60, and 100/80. These mixtures were then kneaded at room temperature for 5 min. (2) The mixtures were further kneaded on the two-roll mill for 5 min at 135°C, followed by cooling off to the room temperature. (3) Also on the two-roll mill, the mixtures were blended with compounding and crosslinking additives, including 5.0 phr zinc oxide, 2.0 phr stearic acid, 0.5 phr dibenzothiazole disulfide, 0.5 phr diphenyl guanidine, 0.2 phr tetramethylthiuram disulfide, and 2.0 phr sulfur; the mixtures were further kneaded at room temperature for 10 min. (4) Finally, the mixtures were hot pressed and vulcanized at 160°C under the pressure of 15 MPa for various periods of time, and then naturally cooled down to room temperature to obtain NBR/AO-60 composites. The amount of time used for the hot pressing/vulcanization was pre-determined for each composite (with its own NBR/AO-60 mass ratio) using a disc rheometer (Model P355C2) purchased from Huanfeng Chemical Technology and Experimental Machine Co. (Beijing, China).

Analysis and characterization

Scanning electronic microscope (SEM) images were taken of the representative fracture surfaces of

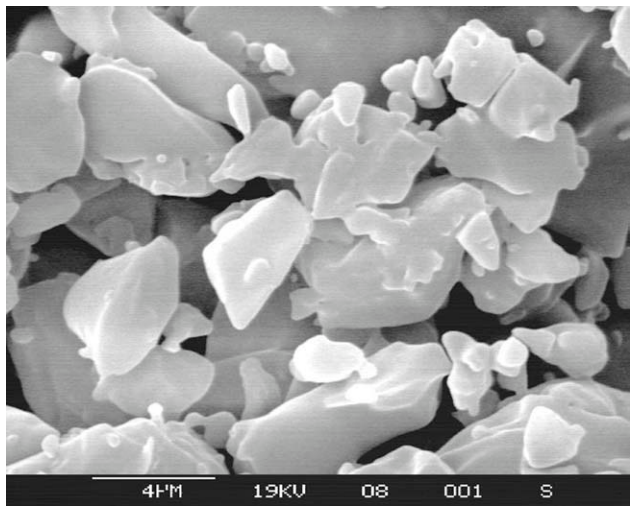

Figure 2 SEM image of as-received AO-60 powder.

AO-60 and NBR/AO-60 blends with the use of an XL-30 field emission SEM (FEI Co., Eindhoven, Netherlands). The SEM specimens were prepared by brittle fracturing the composites in liquid nitrogen.

Differential scanning calorimeter (DSC) measurements were performed on a DSC 204F1 calorimeter (Netzsch Co., Germany). The DSC curves were recorded from −100 to 150°C at a heating rate of 10 °C/min.

Fourier transform infrared (FTIR) spectra were obtained by scanning the specimens in the wavenumber range 400–4000 cm^{-1} with the resolution of 2 cm^{-1} for 128 times. By using the attenuated total reflection (ATR) technique, the FTIR spectra of AO-60 were obtained from the pressed ultra-thin disk specimen made of AO-60 and anhydrous potassium bromide (KBr), whereas the spectra of NBR/AO-60 composites were obtained from the film specimens with a thickness of approximately 1 mm.

Dynamic viscoelasticity measurements were carried out on a dynamic mechanical analyzer (DMA; Viscoanalyzer VA3000, 01dB-Metravib Co., Ltd., France). The specimens were 20-mm long, 6-mm wide, and about 1-mm thick. The temperature dependence of the loss factor tan δ was measured in the range −90 to 150°C at a frequency of 10 Hz and heating rate of 3 °C/min.

Tensile tests of the NBR/AO-60 blends were conducted according to ASTM standard (D412: dumbbell-shaped), and the specimens were tested on an LRX Plus Tensile Tester (Lloyd instruments, Ltd., UK).

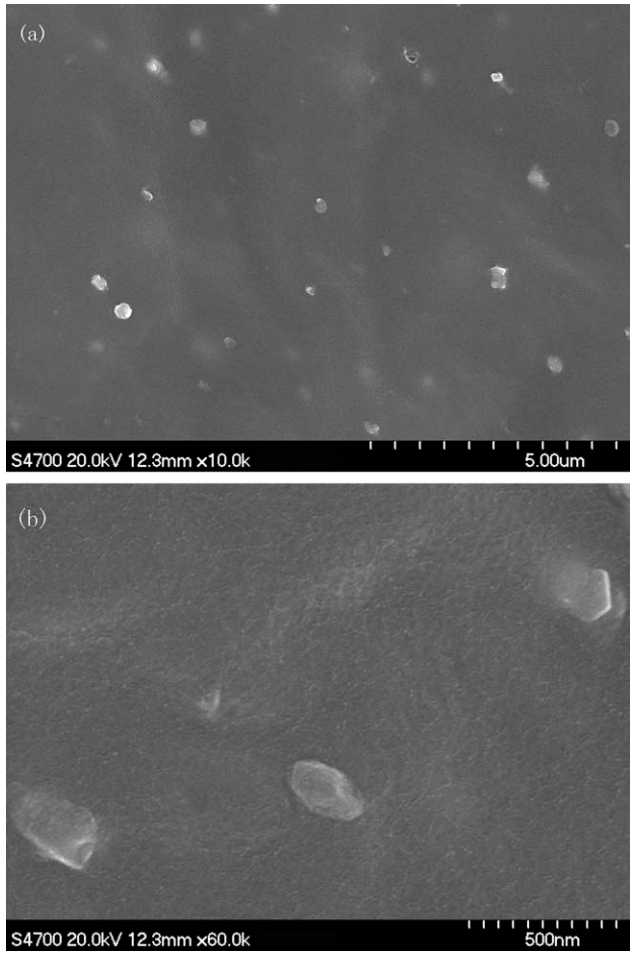

Figure 3 SEM images of representative fracture surfaces of NBR/AO-60 (100/40) composites.

RESULTS AND DISCUSSION

Microscopic morphology of NBR/AO-60 composites

Figure 3 shows the microscopic images of representative fracture surfaces of the NBR/AO-60 (100/40) composite at different magnifications. As shown in Figure 3, the fracture surface is smooth with very few voids/holes. There are few particles at submicron-level size, and the energy dispersive spectrometer (EDS) attached to the SEM indicated that the particles in Figure 3 were actually made of ZnO (an additive for rubber vulcanization). Compared with Figure 2, which shows the shape of AO-60 particles, Figure 3 suggests that the AO-60 molecules are finely dispersed in the NBR matrix in NBR/AO-60 composites. We speculate that the AO-60 molecules in NBR/AO-60 composites primarily exist as tiny particles (a few nanometers in size) or even as molecules/clusters. In the preparation of the NBR/AO-60 composites, the temperatures of kneading and hot pressing were 135°C and 160°C, respectively, which were higher than the AO-60 melting point of 124°C. We believe that the extensive shearing associated with high-temperature kneading and hot pressing can significantly promote the molecular-level mixing of liquid state AO-60 molecules and rubbery state NBR molecules. Intriguingly, the subsequent cooling does not cause phase separation, probably because of the strong intermolecular interactions between AO-60 and NBR molecules. Therefore, NBR/AO-60 composites can be considered as molecular blends, and this assumption is supported by the following DSC, FTIR, and DMA results.

Glass transition of NBR/AO-60 composites

Figure 4 shows the DSC curves of the prepared NBR/AO-60 composites with various mass ratios of NBR/AO-60. The curves of neat NBR and AO-60 (both as-received and quenched) are also included for comparison purposes. As shown in Figure 4, the as-received AO-60 powder is crystalline and has a melting temperature of about 124.0°C, and the neat NBR has a glass transition temperature of about −24.3°C. After the as-received AO-60 was heated to

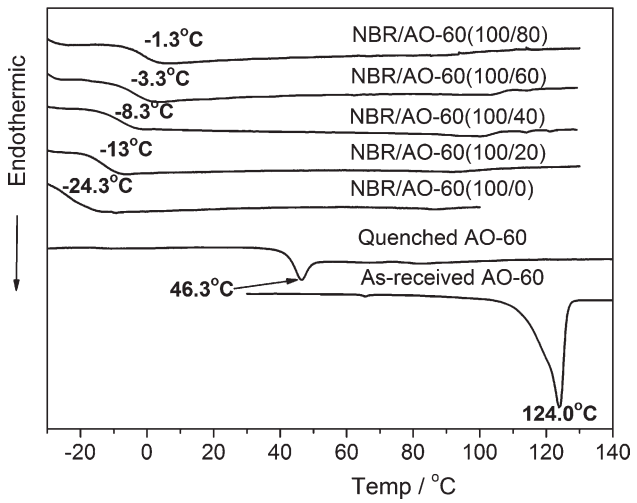

Figure 4 DSC curves of AO-60 (as-received and quenched) and NBR/AO-60 composites.

160°C and quickly quenched to room temperature, amorphous AO-60 with a glass transition temperature around 46.3°C was obtained. The DSC curve of each NBR/AO-60 composite shows only one glass transition temperature (T_g) for the temperatures tested, which corresponds to the NBR matrix, and the T_g shifts gradually from −24.3°C to −1.3°C as the AO-60 content increases from 0 phr to 80 phr. At the same time, none of the NBR/AO-60 composites shows the AO-60 melting peak.

As discussed earlier, in the preparation of the NBR/AO-60 composites, the temperatures of kneading and hot pressing were higher than the AO-60 melting point. Therefore, the AO-60 molecules were amorphous in the NBR/AO-60 composites, and as a result there is no AO-60 melting peak in the DSC curves. The question then arises as to why there is no glass transition of AO-60 in the DSC curves of NBR/AO-60 composites. As mentioned earlier, the processing temperature used in the preparation of NBR/AO-60 composites was higher than the AO-60 melting point. Hence the AO-60 was in the liquid state in the preparation of the NBR/AO-60 composites and finely dispersed in the NBR matrix. As a result, the NBR/AO-60 composites do not display the glass transition corresponding to the AO-60 phase. The reason for the increase of the T_g of NBR/AO-60 composites with increasing AO-60 content is the formation of strong intermolecular interactions between the AO-60 molecules and NBR matrix. With increasing content of AO-60 in the NBR/AO-60 composites, the intermolecular interactions between the AO-60 molecules and NBR matrix get stronger. As the movement of macromolecular chains becomes more difficult, the glass transition temperature of NBR increases steadily. To sum up, the NBR/AO-60 system does not show the characteristics of two-phase materials, as a result of the molecular-level dispersion of AO-60 in NBR and the formation of strong intermolecular interactions between AO-60 and NBR. These DSC results are consistent with the SEM results reported earlier.

FTIR spectroscopy is a suitable technique for investigating specific intermolecular interactions. Figure 5 shows the FTIR spectra for the quenched AO-60, NBR, NBR/AO-60 (100/40), and NBR/AO-60 (100/80) composites in the wavenumber range 4000–3000 cm^{-1}. The spectrum for the quenched AO-60 indicates the significant absorptions at 3638 cm^{-1} and 3440 cm^{-1}, which are assigned to OH vibrations caused by free OH and OH—OH interactions (hydrogen bonding) respectively, between AO-60 molecules.[16] For the pure vulcanized NBR sample, no band appears in the wavenumber range 4000–3000 cm^{-1}. However, for each of the NBR/AO-60 (100/40) and NBR/AO-60 (100/80) composites, a characteristic band appears, corresponding to the quenched AO-60. Compared with the characteristic band for quenched AO-60, the band at about 3638 cm^{-1} (assigned to free OH) shows no obvious shift. Moreover, the band assigned to OH—OH interactions shifts from 3638 to 3424 cm^{-1}. This shift can be attributed to hydrogen bonding between the -OH groups of AO-60 and the -CN groups of NBR. Furthermore, we can see that the wavenumber for the hydrogen bonding between AO-60 and NBR (OH—CN, 3424 cm^{-1}) is lower than that for the hydrogen bonding in quenched AO-60 (OH—OH, 3440 cm^{-1}), indicating that the bonding energy of the former is stronger than that of the latter. That is to say, the intermolecular interactions between the -OH groups of AO-60 and the -CN groups of NBR are stronger than those between AO-60 molecules. The formation of stronger intermolecular interactions in the NBR/AO-60 composites could limit the

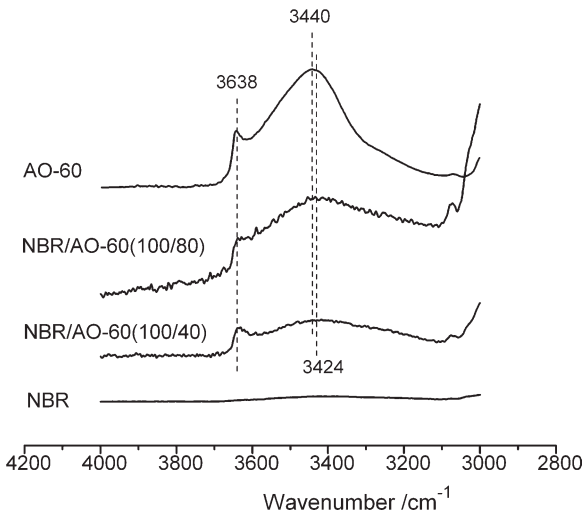

Figure 5 FTIR spectra of the quenched AO-60 and NBR/AO-60 composites.

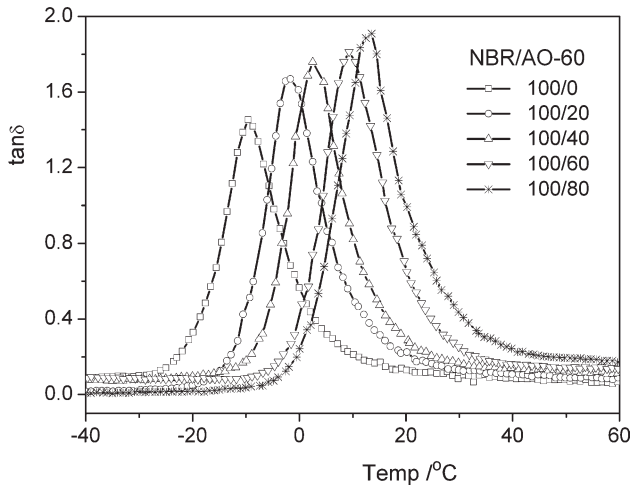

Figure 6 Temperature dependence of loss tangent (tan δ) values for NBR and NBR/AO-60 composites with different mass ratios of NBR/AO-60.

molecular motion of NBR and increase the friction between NBR chains. Consequently, the T_g of the NBR/AO-60 composites increases substantially over that of NBR, and the damping properties improve significantly.

Dynamic mechanical properties of NBR/AO-60 composites

Figure 6 shows the temperature dependence of the loss tangent (tan δ) values for NBR and NBR/AO-60 composites with different mass ratios of NBR/AO-60. It can be seen that each NBR/AO-60 composite shows only one tan δ peak. With increasing amount of AO-60 in the composites, the tan δ peak gradually shifts to higher temperatures. From the DSC and FTIR analyses presented above, the functional groups of AO-60 form hydrogen bonds with the polar groups on the NBR macromolecular chain, and macromolecular chain movement is thus limited. With increasing AO-60 content, the intermolecular forces between NBR and AO-60 gradually increase, the movement of macromolecular chains becomes more difficult, and the glass transition temperature of NBR/AO-60 increases. The T_g of every NBR/AO-60 composite is significantly higher than that of pure NBR. The loss peak of every NBR/AO-60 composite is larger than that of pure NBR, and the loss peak of NBR/AO-60 increases with increasing AO-60 content.

Table I shows the damping properties of NBR/AO-60 composites. With the AO-60 content increasing, the loss peak value of NBR/AO-60 gradually increases from 1.45 to 1.91, and the temperature range between tan $\delta \geq 0.3$ and tan $\delta \geq 0.6$ becomes gradually wider. Temperature curve (TA; the area under the tan δ versus temperature curve) is commonly used for characterizing the damping properties of rubber.[19] The larger the TA value, the better the damping properties of material. The TA values in Table I show that when the AO-60 amount increases from 0 phr to 80 phr, the TA value of NBR/AO-60 composites increases from 32.9°C to 51.5°C. Both the loss peak and TA values indicate that the damping properties of NBR/AO-60 composites improve with increasing AO-60 content.

Figure 7 shows the temperature dependence of the storage modulus (E') of the prepared NBR/AO-60 composites. Every storage modulus curve displays only one transition, and the plot of E' versus temperature moves toward higher temperatures with increasing amount of AO-60. The shift towards high temperatures can be attributed to the fine dispersion of AO-60 in the NBR matrix and the strong hydrogen bonding between AO-60 and NBR. As the amount of AO-60 increases, the storage modulus in the glassy region increases whereas the storage modulus in the rubbery region decreases. The increase of the storage modulus in the glassy region is due to the reinforcement of the NBR matrix by AO-60. The storage modulus decreases in the rubbery region because AO-60 becomes soft and acts as a plasticizer when the temperature exceeds the T_g (46.3°C) and approaches the melting temperature (124°C) of AO-60.

Static mechanical properties of NBR/AO-60 composites

Figure 8 shows the tensile stress–strain curves of the prepared NBR/AO-60 composites with various NBR/AO-60 mass ratios, and Table II summarizes

TABLE I
Damping Properties of NBR/AO-60 Composites

NBR/AO-60	tan δ_{max} Value	tan δ_{max} T (°C)	Temperature range of tan $\delta \geq 0.3$ (°C)	Temperature range of tan $\delta \geq 0.6$ (°C)	TA (°C)
100/0	1.45	−9.6	−20.6 to +5.9	−16.2 to −0.5	32.9
100/20	1.67	−1.7	−11.6 to +15.4	−8.8 to +8.2	36.3
100/40	1.76	2.2	−7.2 to +20.3	−4.4 to +12.6	42.2
100/60	1.81	9.3	−1.3 to +28.0	+1.8 to +20.6	46.9
100/80	1.91	13.6	+0.8 to +35.2	+4.1 to +25.7	51.5

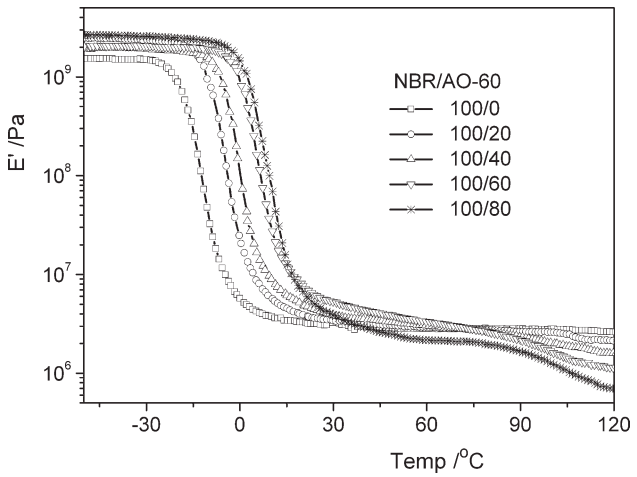

Figure 7 Temperature dependence of storage modulus (E') for NBR and NBR/AO-60 composites with different mass ratios of NBR/AO-60.

the acquired data. It can be seen from Figure 8 that the tensile strength and elongation at break of NBR/AO-60 composites increases with increasing amount of AO-60, especially at mass ratios NBR/AO-60 above 100/40. However, the tensile modulus at 100% or 300% elongation of the NBR/AO-60 composites decreases with increasing amount of AO-60. As is well known, crosslinking has a significant impact on the tensile strength of rubber. With the amount of AO-60 increasing, the relative amount of NBR in the NBR/AO-60 composites decreases, and the crosslinking of NBR is affected to some extent. As a kind of physical force, hydrogen bonding between AO-60 and NBR is much weaker than the chemical crosslinking in vulcanized NBR. Therefore, the tensile modulus at 100% or 300% elongation of the composites is lower than the corresponding value of neat NBR. At the same time, hydrogen bonds are reversible in the sense that they are easy to form and

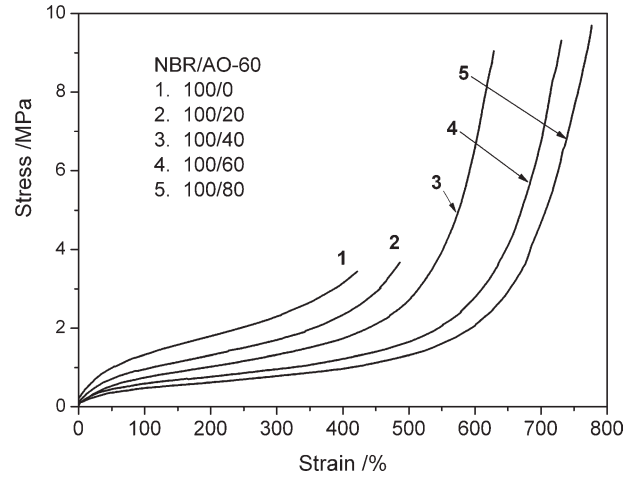

Figure 8 Stress/strain curves of NBR and NBR/AO-60 composites with different mass ratios of NBR/AO-60.

TABLE II
Mechanical Properties of NBR/AO-60 Composites

Properties	Loadings of AO-60				
	0 phr	20 phr	40 phr	60 phr	80 phr
Hardness (Shore A)	50	52	54	57	62
Modulus at 100% (MPa)	1.33	0.96	0.75	0.59	0.48
Modulus at 300% (MPa)	2.30	1.70	1.33	0.96	0.78
Tensile strength (MPa)	3.0	3.8	9.2	9.5	9.8
Elongation at break (%)	422	487	628	730	777
Permanent set (%)	4	4	4	4	8

destroy. In the drawing process, the macromolecular chains of NBR tend to align along the tensile direction. The hydrogen bonding between AO-60 and NBR is a process of repeated destruction and formation, which consumes a lot of energy and brings the orientation effect to the NBR/AO-60 composites. As a result, the tensile strength and elongation at break of NBR/AO-60 composites increase. Table II also lists the hardness and permanent set of the NBR/AO-60 composites. The results indicate that the composites have small permanent set and low hardness, both very important for application purposes.

CONCLUSIONS

NBR/AO-60 composites were successfully prepared in this study. The crystalline AO-60 turns amorphous, and most of the AO-60 molecules can be uniformly dispersed in the NBR matrix. The glass transition temperature (T_g) of NBR/AO-60 composites increases gradually with increasing AO-60 content. The T_g increase can be attributed to strong hydrogen bonding between the AO-60 molecules and the NBR matrix. Unlike pure NBR, each NBR/AO-60 rubber composite has only one glass transition with a high loss factor. With increasing AO-60 content, the loss peak shifts to high temperatures, the loss factor increases from 1.45 to 1.91, and the TA value also increases significantly, all the results of good compatibility and strong intermolecular interactions between NBR and AO-60. Furthermore, all NBR/AO-60 composites exhibit high glass transition temperature, high tensile strength, and other desirable mechanical properties, and thus have excellent prospects for damping material applications.

References

1. Wang, Y. Y.; Chen, X. R.; Huang, G. S. Mater Rev 2004, 18, 54.
2. Mao, X. D.; Xu, S. A.; Wu, C. F. Polym Plast Technol Eng 2008, 47, 209.
3. Kuo, S. W.; Chang, F. C. Macromol Chem Phys 2001, 202, 3112.
4. Wu, H. D.; Chu, P. P.; Ma, C. C.; Chang, F. C. Macromolecules 1999, 32, 3097.

5. Perera, M. C. S.; Ishak, Z. A. M. Eur Polym J 2001, 37, 167.
6. Yamada, N.; Shoji, S.; Sasaki, A.; Nagatani, A.; Yamaguchi, K.; Kohjiya, S.; Hashim, A. J Appl Polym Sci 1999, 71, 855.
7. Qin, C. L.; Cai, W. M.; Cai, J.; Tang, D. Y.; Zhang, J. S.; Qin, M. Mater Chem Phys 2004, 85, 402.
8. Manoj, N. R.; Ratna, D.; Dalvi, V. Chandrasekhar, L.; Patri, M.; Chakraborty, B. C.; Deb, P. C. Polym Eng Sci 2002, 42, 1748.
9. Wu, C. F.; Yamagishi, T.; Nakamoto, Y; Ishida, S.; Nitta, K.; Kubota, S. J Polym Sci Part B: Polym Phys 2000, 38, 1341.
10. Wu, C. F.; Mori, K.; Otani Y.; Namiki, N.; Emi, H. Polymer 2001, 42, 8289.
11. Wu, C. F. J Polym Sci Part B: Polym Phys 2001, 39, 23.
12. Wu, C. F.; Yamagishi, T.; Nakamoto, Y. Polym Int 2001, 50, 1095.
13. Zhao, X. Y.; Xiang, P.; Tian, M.; Fong, H.; Jin, R. G.; Zhang, L. Q. Polymer 2007, 48, 6056.
14. Zhao, X. Y.; Xiang, P.; Zhang, L. Q. Acta Mater Compos Sinica 2007, 24, 44.
15. Zhao, X. Y.; Lu, Y. L.; Xiao, D. L.; Wu, S. Z.; Zhang, L. Q. Macro Mater Eng 2009, 294, 345.
16. Xiao, D. L.; Zhao, X. Y.; Xiang, P.; Zhang, L. Q. J Appl Polym Sci 2010, 116, 2143.
17. Xiang, P.; Zhao, X. Y.; Xiao, D. L.; Zhang, L. Q. J Appl Polym Sci 2008, 109, 106.
18. Xiang, P.; Xiao, D. L.; Zhao, X. Y.; Zhang, L. Q. Acta Mater Compos Sinica 2007, 24, 44.
19. Fay, J. J.; Murphy, C. J.; Thomas, D. A.; Sperling, L. H. Polym Eng Sci 1991, 31 1731.